The evaluation and analysis of the optical properties of wurtzite III-nitride semiconductor thin films via UV-VIS reflectance spectroscopy

Zaheer Ahmad

Department of Physics and Astronomy, Georgia State University, Atlanta, Georgia 30303, USA

III-nitride semiconductor thin films grown over c-plane Al_2O_3 have been analyzed by simulating the reflectance of each of GaN, InN and AlN. The reflectance simulations have been performed by using a model dielectric function which is essentially a modified Lorentz oscillator dielectric function described in terms of three most dominant transitions in the band structure of each of iii-nitride semiconductor. Thin film characteristics have been derived by a comparison of the simulated reflectance with the experimentally recorded reflectance for each of the samples.

I.   INTRODUCTION

Due to the peculiar optoelectronic and structural features of group III-nitride compound semiconductors, indium nitride, gallium nitride, aluminum nitride and their alloys such as AlGaN and InGaN are of vital importance in high power and high-speed optoelectronic devices. [1-3]

Most of the III-nitride devices are manufactured by patterning (e.g. lithography) on the multilayer heterostructures of these compound semiconductors. Hence a thorough understanding of the optical properties of semiconducting layers is needed for in-depth knowledge and control over the resulting optoelectronic device's performance.

This paper presents the structural analysis via normal incidence reflectance spectroscopy (NIRS), of the GaN, InN and AlN thin films grown over c-plane Al_2O_3 by conventional MOCVD and Migration enhanced plasma assisted MOCVD.

The theoretical reflectance for each of the InN, GaN, and AlN thin films is simulated using Goldhahn's dielectric functions [4] in a restricted energy range, and then a comparison of the simulated and experimental reflectance yields the film thickness and RMS roughness of the film.

II.   PROPERTIES OF WURTZITE III-NITRIDES
a)   Structural properties of the Wurtzite iii-nitrides

The group III nitrides crystallize as three crystal structures namely wurtzite, zinc blende, and rock salt. Wurtzite is thermodynamically most stable and energetically most favorable structure for bulk GaN, AlN and InN. [6]

The c/a ratio of the wurtzite structure is 8/3 since it has a hexagonal unit cell. Essentially a wurtzite structure is an overlap of two hexagonal close-packed sublattices displaced along the c-axis by an amount u = 1.633. Each of these sublattices contains four atoms per unit cell, and four nitrogen atoms tetrahedrally surround every group III atom. The actual nitrides deviate from the above-mentioned ideal structure, which is signified by the 'c∕a' ratio or 'u' value [7]

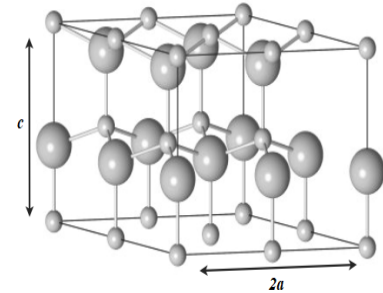The wurtzite crystal structure in real and reciprocal space is shown in figures 1 and 2 respectively.

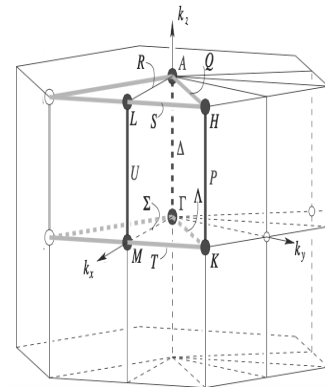**FIG** 1. The wurtzite structure[5]

FIG 2. Wurtzite structure in reciprocal space. Brillouin zone with all the high symmetry points is shown. [5]

b) Optical properties of the Wurtzite iii-nitrides

All the III-nitrides are direct bandgap semiconductors, having the minimum of the conduction band and the maximum of the valence band aligned with other at the Γ point on the k-axis. The joint density of states (JDOS) function for these materials experiences singularities at the critical points in the Brillouin zone. The relative gradient between the band is zero at these points. [8]

These singularities are termed as Van Hove singularities. Van Hove singularities are the location on k-axis of the dominant interband transitions. The shape of the dielectric function of the material is strongly dependent upon these transitions. Figure 3 summarizes the band structure for III-nitrides.
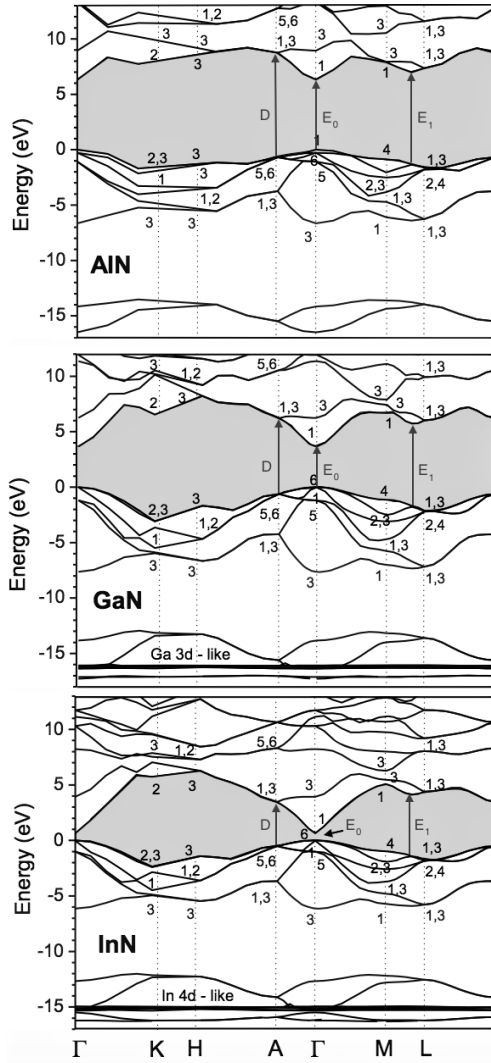

FIG 3. The band structure of AlN, GaN and, InN [5]

III. THEORY
a) Reflectance of a multilayer structure

For an n-layer stack, at the interface between (n-1)[th] and nth layer, the reflected and transmitted amplitudes v_n and w_n respectively of the wave are linked via the equations 1 and 2.

$$v_{n+1} = \left(v_n e^{i\delta_n}\right)t_{n.n+1} + w_{n+1}r_{n+1,n} \quad \text{--- 1}$$

$$w_n e^{-i\delta_n} = w_{n+1}t_{n+1.n} + \left(v_n e^{i\delta_n}\right)r_{n,n+1} \quad \text{---2}$$

Here "δ_n" is the phase change that the wave experiences while travelling through the layer "n" and is defined as[8]

δ_n = (layer thickness)×(k$_z$ for the forward travelling wave)

While the Fresnel "r" and "t" coefficients for s and p polarization are given by the equations 3, 4, 5, and 6[9]

$$r^p_{n,n+1} = \frac{\epsilon_{n+1}\sqrt{\epsilon_n - \epsilon_0 Sin^2\theta} - \epsilon_n\sqrt{\epsilon_{n+1} - \epsilon_0 Sin^2\theta}}{\epsilon_{n+1}\sqrt{\epsilon_n - \epsilon_0 Sin^2\theta} + \epsilon_n\sqrt{\epsilon_{n+1} - \epsilon_0 Sin^2\theta}} \quad \text{---- 3}$$

$$r^s_{n,n+1} = \frac{\sqrt{\epsilon_n}\,cos\theta - \sqrt{\epsilon_{n+1} - \epsilon_0 Sin^2\theta}}{\sqrt{\epsilon_n}\,cos\theta + \sqrt{\epsilon_{n+1} - \epsilon_0 Sin^2\theta}} \quad \text{----- 4}$$

$$t^p_{n,n+1} = \frac{2\sqrt{\epsilon_{n+1}}\sqrt{\epsilon_{n+1} - \epsilon_0 Sin^2\theta}}{\epsilon_{n+1}cos\theta + \sqrt{\epsilon_n}\sqrt{\epsilon_{n+1} - \epsilon_0 Sin^2\theta}} \quad \text{----- 5}$$

$$t^s_{n,n+1} = \frac{2\sqrt{\epsilon_n - \epsilon_0 Sin^2\theta}}{\sqrt{\epsilon_n - \epsilon_0 Sin^2\theta} + \sqrt{\epsilon_{n+1} - \epsilon_0 Sin^2\theta}} \quad \text{----- 6}$$

The "ϵ" in the equations 3 to 6 is the dielectric function of the corresponding layer and 'θ' is the angle of incidence with normal to the top layer in the multilayer stack.

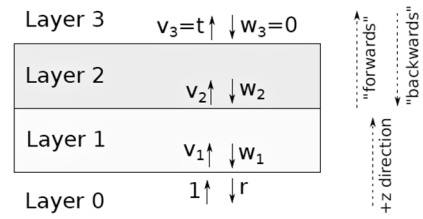Figure 4[8] describes the normal incidence geometry used in this study for the reflectance measurement.

FIG 4. A four-layer stack with layers "0" and "3" being air/ambient, the layer "1" is sapphire substrate while "2" is III-nitride film in this study

b) Model of dielectric function

The Goldhahn's model dielectric function [4] (MDF) is partially used in a restricted energy range to simulate the optical properties of the iii-nitride thin films.

$$\epsilon(\omega) = \sum_{j=D,1,0}\left\{\frac{A_j^2}{(E_j^2-\hbar^2\omega^2-i\hbar\omega\Gamma_j)}\right\} +$$

$$\frac{1}{\pi}A_l\left(\ln\left\{\frac{E_P^2-(\hbar\omega+i\Gamma_l)^2}{(E_o^2-(\hbar\omega+i\Gamma_l)^2}\right\} + \frac{A_pE_p}{(E_p^2-(\hbar\omega+i\Gamma_l)^2}\right) \text{-7}$$

MDF is described as modified Lorentz oscillators [12-15] in terms of the most dominant transitions labelled as E_1, E_O and D in the band diagram in figure 3. The imaginary part added to the photon energy takes care of the singularities at the bandgap, and E_p is the background term that takes care of the higher energy interband transitions. [4,10]

Table 1 summarizes established the numerical values of the parameters used in equation 7 to model the DF of iii-nitride films. [10]

	GaN	AlN	InN
A_1	7.53	7.00	4.9
E_1	7.00	7.90	5.45
Γ_1	0.90	0.80	0.82
A_D	4.80	0.50	3.60
E_D	6.20	8.20	4.89
Γ_D	5.40	0.50	0.80
A_o	0.33	0.33	0.01
E_o	3.44	6.21	0.72
Γ_o	0.06	0.06	0.09
A_p	61.00	44.00	13.00
E_p	8.80	9.20	6.20
A_l	1.50	1.60	2.07
Γ_l	0.006	0.005	0.04
C	0.40	1.40	2.95

Table 1. Established parameters for MDFP

IV.   EXPERIMENTAL DETAILS

One sample of each gallium nitride, indium nitride and aluminum nitride are used in this study. The gallium nitride and aluminum nitride samples are grown using traditional metalorganic chemical vapor deposition, while the indium nitride is grown via plasma-assisted metalorganic chemical vapor deposition technique.

The reflectance spectra of all the samples used in this study are recorded in backscattering geometry as shown in figure 4, measured with a fiber optic spectrometer using a back-thinned 2D FFT-CCD detector. The spectrometer used is highly sensitive in a range of ~165-1100 nm and is therefore perfect for deep-UV (vacuum UV), UV-Vis and Vis-NIR measurements. [11] All the spectra were acquired at three-second integrations each with a range of 165nm to 1100 nm.

V.   RESULTS AND DISCUSSION

Figure 5, 6 and 7 show three sets of the simulated reflectance for gallium nitride, indium nitride, and aluminum nitride films over the restricted energy range of 2.26eV to 3.26eV. The main reason for limiting the energy range for reflectance simulations is to avoid all the transitions at the bandgap of either of the gallium nitride, aluminum nitride or indium

nitride, for which if included would require to change the proposed MDF for the iii-nitride thin films considerably.

It is evident from the figures 5-7 that the number of fringes increases with the increased film thickness for each of the GAN, AlN, and InN as follows from the primary optics [16-19] of thin film structures. But the reflectance spectra of the films with the same thickness of the different materials must be different since their dielectric functions are not the same.
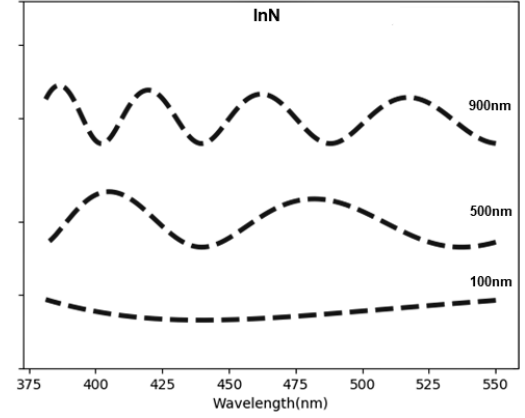

FIG 5. Simulated reflectance vs. wavelength based on proposed MDF for three InN films with different thicknesses
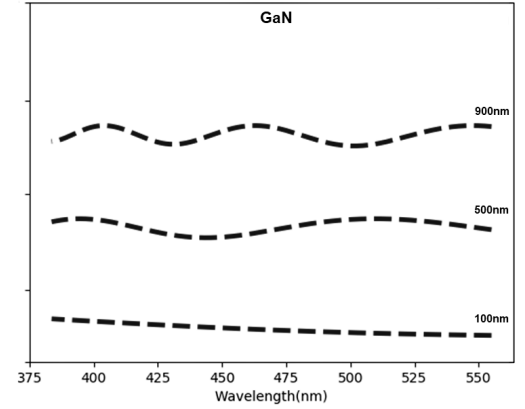

FIG 6. Simulated reflectance vs. wavelength based on proposed MDF for three GaN films with different thicknesses

The structural analysis of all the iii-nitride samples used in this study has been done by comparing the simulated reflectances based upon MDF and the experimentally recorded reflectance for the film thickness and surface roughness of the films.

It has been found for all the three samples' whose thickness, and surfaces roughness have been extracted, the simulated and experimental reflectance were in agreement between 94 to 99.99 %, figures 8, 10 and 12.
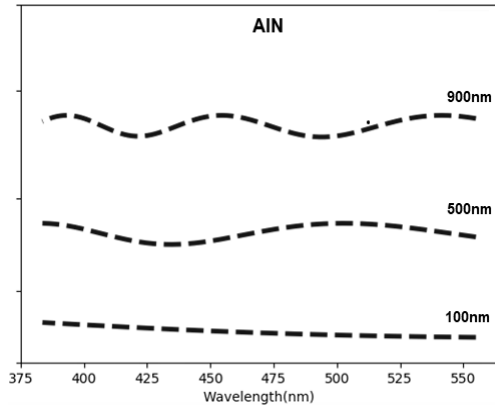
FIG 7. Simulated reflectance vs. wavelength based on proposed MDF for three GaN films with different thicknesses
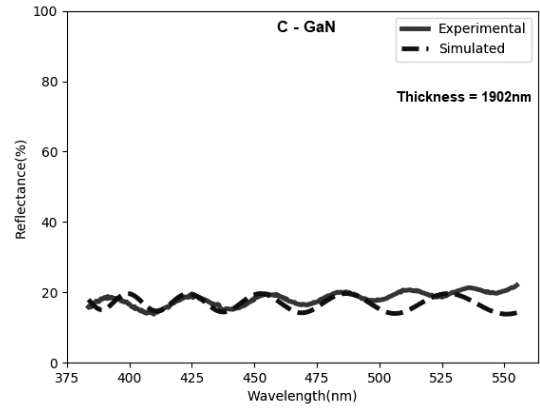

FIG 10. Simulated and experimental reflectance vs. wavelength GaN film
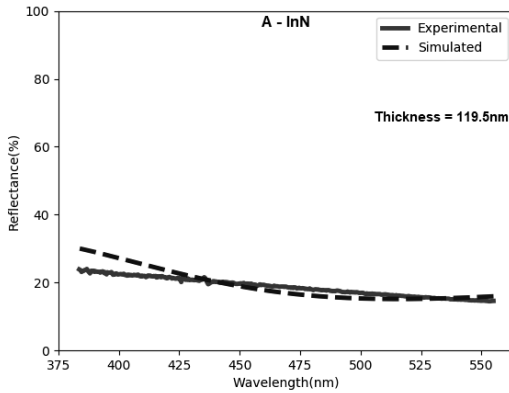

FIG 8. Simulated and experimental reflectance vs. wavelength InN film
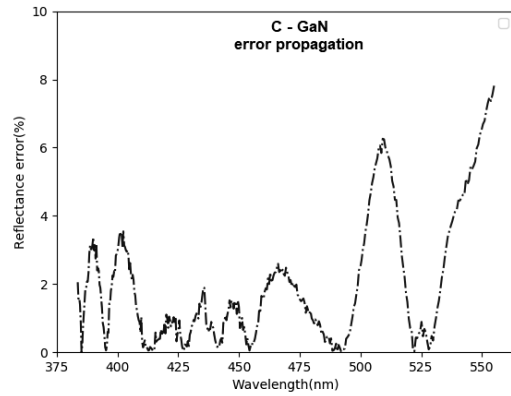

FIG 11. Error propagation with wavelength for C-GaN
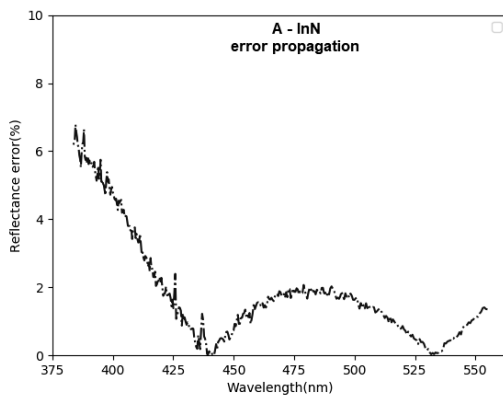

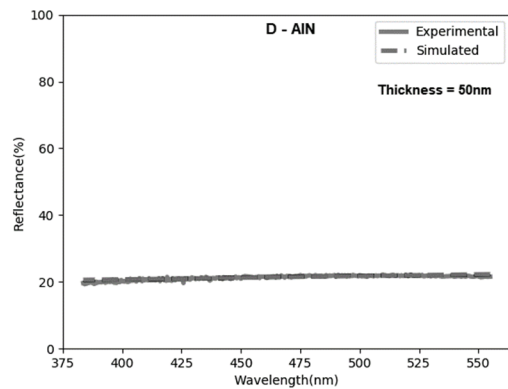FIG 9. Error propagation with wavelength for A-InN

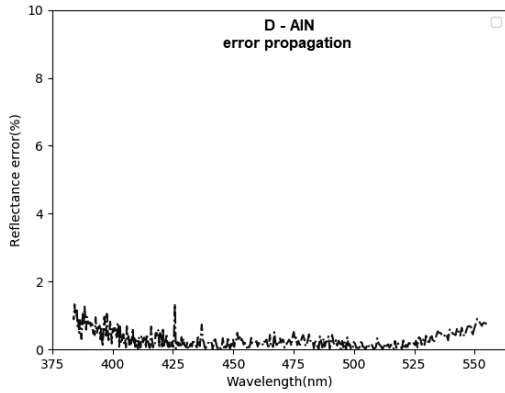FIG 12. Simulated and experimental reflectance vs. wavelength AlN film

FIG 13. Error propagation with wavelength for D-AlN

The difference or error of the simulated reflectance with the experimental varies between 0 to 6% over the range 380nm to 550nm wavelength figures 14 to19.

The RMS surface roughness of the iii-nitride films predicted by the simulations are linearly related to the ones obtained from actual AFM scans and is shown in fig 14.
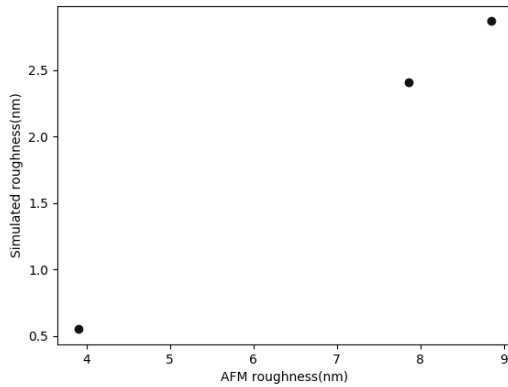

FIG 14. Simulated vs. measured surface rouhness

For all three samples used in the study, the ratio of the predicted surface roughness to the one measured through AFM remain same at 0.4.

VI. CONCLUSIONS

The structural analysis of III-nitrides semiconductor thin films via the reflectance simulations based on MDF has been successfully performed. The surface roughness predicted by the simulations for all three samples used in this study is found to be 0.4 times the actual surface roughness measured by the AFM.

[1] Bhuiyan, Ashraful Ghani, Akihiro Hashimoto, and Akio Yamamoto. "Indium nitride (InN): A review on growth, characterization, and properties." *Journal of Applied Physics* 94.5 (2003): 2779-2808.

[2] Butcher, K. Scott A., and T. L. Tansley. "InN, latest development and a review of the band-gap controversy." *Superlattices and Microstructures* 38.1 (2005): 1-37.

[3] Davydov, V. Yu, and A. A. Klochikhin. "The electron and vibration states of InN and In x Ga 1-x N solid solutions." *Fizika i Tekhnika Poluprovodnikov* 38.8 (2004): 897-936.

[4] Goldhahn, Riidiger, et al. "Optical constants of bulk nitrides." *Nitride Semiconductor Devices: Principles and Simulation* (2007): 95.

[5] Carvalho, Luiz Claudio de. *Modeling of III-nitride Alloys by Ab-initio Methods*. Diss. 2012.

[6] Ferreyra R.A., Zhu C., Teke A., Morkoç H. (2017) Group III Nitrides. In: Kasap S., Capper P. (eds) *Springer Handbook of Electronic and Photonic Materials. Springer Handbooks. Springer, Cham*

[7] C.-Y. Yeh, Z. Lu, S. Froyen, A. Zunger: Zinc-blende–wurtzite polytypism in semiconductors, Phys. Rev. B **46**(16), 10086 (1992)

[8] Byrnes, Steven J. "Multilayer optical calculations." *arXiv preprint arXiv:1603.02720* (2016).

[9] Heavens, Oliver S. *Optical properties of thin solid films*. Courier Corporation, 1991.

[10] Vernon, Mark. "Approximation and Analysis of Optical Properties of Group-III Nitride Multilayer Heterostructures." Georgia State University, 2015.

[11] "Maya2000 Pro (Custom)." *Ocean Optics, oceanoptics.com/product/maya2000-pro-custom/*.

[12] Tompkins, Harland, and Eugene A. Irene. *Handbook of ellipsometry*. William Andrew, 2005.

[13] Jellison Jr, G. E., and F. A. Modine. "Parameterization of the optical functions of amorphous materials in the interband region." *Applied Physics Letters* 69.3 (1996): 371-373.

[14] Bunshah, Rointan Framroze, ed. *Handbook of deposition technologies for films and coatings: science, technology, and applications*. William Andrew, 1994.

[15] Djurišić, Aleksandra B., and E. Herbert Li. "Modeling the index of refraction of insulating solids with a modified Lorentz oscillator model." *Applied optics* 37.22 (1998): 5291-5297.

[16] Macleod, H. Angus, and H. Angus Macleod. *Thin-film optical filters*. CRC press, 2010.

[17] Eckertova, Ludmila. *Physics of thin films*. Springer Science & Business Media, 2012.

[18] Heavens, Oliver Samuel. *Thin film physics*. Methuen, 1970.

[19] Niedermayer, Rolf, and Herbert Mayer, eds. *Basic problems in thin film physics*. Göttingen: Vandenhoeck & Ruprecht, 1966.